Published in final edited form as:
Biochemistry. 2010 February 16; 49(6): 1331–1337. doi:10.1021/bi901810u.

Eribulin Binds at Microtubule Ends to a Single Site on Tubulin to Suppress Dynamic Instability†

Jennifer A. Smith[‡], **Leslie Wilson**[‡], **Olga Azarenko**[‡], **Xiaojie Zhu**[§], **Bryan M. Lewis**[§], **Bruce A. Littlefield**[Δ,#], and **Mary Ann Jordan**[*,‡]

[‡]Department of Molecular, Cellular, and Developmental Biology and the Neuroscience Research Institute, University of California Santa Barbara, Santa Barbara, California 93106

[§]Process Development, Eisai Research Institute, Andover, Massachusetts, 01810

[Δ]Scientific Administration, Eisai Research Institute, Andover, Massachusetts, 01810

Abstract

Eribulin mesylate (E7389), a synthetic analog of the marine natural product halichondrin B, is in Phase III clinical trials for the treatment of cancer. Eribulin targets microtubules, suppressing dynamic instability at microtubule plus ends through an inhibition of microtubule growth with little or no effect on shortening. Using [^{3}H]eribulin, we found that eribulin binds soluble tubulin at a single site; however, this binding is complex with an overall K_d of 46 μM, but also showing a real or apparent very high affinity (K_d, 0.4 μM) for a subset of 25% of the tubulin. Eribulin also binds microtubules with a maximum stoichiometry of 14.7 ± 1.3 molecules per microtubule (K_d, 3.5 μM), strongly suggesting the presence of a relatively high affinity binding site at microtubule ends. At 100 nM, the concentration that inhibits microtubule plus end growth by 50%, we found that one molecule of eribulin is bound per 2 microtubules, indicating that the binding of a single eribulin molecule at a microtubule end can potently inhibit its growth. Eribulin does not suppress dynamic instability at microtubule minus ends. Pre-incubation of microtubules with 2 or 4 μM vinblastine induced additional lower affinity eribulin binding sites, most likely at splayed microtubule ends. Overall, our results indicate that eribulin binds with high affinity to microtubule plus ends and thereby suppresses dynamic instability.

Keywords

eribulin; halichondrin; tubulin; microtubule; binding

Eribulin mesylate is a tubulin/microtubule-targeting chemotherapeutic drug that inhibits the proliferation of multiple cancer cell types (1,2). It is a synthetic analog of the natural compound, halichondrin B (Fig. 1A), initially isolated from the sea sponge *Halichondria okadai* (3). Eribulin is currently in Phase III clinical trials for the treatment of metastatic breast cancer. Phase I and Phase II clinical trials have demonstrated that eribulin is active in heavily pre-treated individuals while maintaining a tolerable therapeutic index, with the most frequent adverse effects being neutropenia and fatigue (4-6). Neuropathy, a common dose-limiting toxicity of other microtubule-targeting drugs like paclitaxel and some vinca alkaloids (7-9), has a low incidence in eribulin-treated patients, and no grade 4 neuropathy occurred (4-6).

†Supported by grants from Eisai Research Institute, NIH CA 57291, NS13560

[#]Current address: Harvard Medical School, Landmark 22A-West, 401 Park Drive, Boston, MA 01810
[*]Molecular Cellular and Developmental Biology, UC Santa Barbara, Santa Barbara, CA 93106, Phone: (805) 893-5317; Fax: (805) 893-5081, jordan@lifesci.ucsb.edu

Eribulin exerts its anticancer properties through a novel action on tubulin and microtubules (1,10-12). In MCF7 cells, eribulin inhibited microtubule dynamic instability at low concentrations and induced depolymerization of the microtubule network at high concentrations ($10 \times IC_{50}$ for inhibition of cell proliferation) (11). At significantly lower eribulin concentrations, eribulin potently inhibited microtubule dynamics, resulting in prolonged mitotic arrest and subsequent apoptosis [for a review of microtubule structure and dynamic instability, see (13,14)]. Eribulin binds at or near the vinca domain, a region that is located at the interface of two tubulin heterodimers when arranged end-to-end and overlaps the exchangeable GTP site on β-tubulin (2,10,15-17). Eribulin inhibits vinblastine binding to free tubulin non-competitively with an apparent K_i of 1.9 μM, and it inhibits GTP hydrolysis and exchange (2), as do most compounds that bind in the vinca domain (16).

Microtubules undergo complex growth and shortening events, termed dynamic instability. Microtubule-targeting drugs inhibit dynamic instability by altering tubulin addition and loss parameters, which in turn inhibits the ability of a cell to undergo successful mitotic division (14). Eribulin's effects on dynamic instability are novel, in that eribulin suppresses the growth parameters at microtubule plus ends without affecting microtubule shortening parameters, both in cells and in a purified *in vitro* system (11), resulting in an overall decrease in dynamicity. Based on these findings, we hypothesized that eribulin preferentially binds tubulin at microtubule ends, thus blocking the addition of tubulin dimers to a growing end.

To determine the mechanism by which eribulin suppresses microtubule growth, we examined the binding of eribulin to soluble tubulin and to polymerized microtubules using radiolabeled eribulin. We also examined the effects of eribulin on steady-state microtubule polymer mass and on the dynamic instability of minus ends. Our results indicate that eribulin binds to a single site on tubulin heterodimers, and that eribulin binds to microtubule ends, most likely at plus ends. We found that vinblastine binding to microtubules inhibited eribulin binding at low eribulin concentrations, but also appeared to open up additional, low affinity binding locations for eribulin, at either one or both microtubule ends.

MATERIALS AND METHODS

Eribulin

Eribulin [NSC-707389; previously E7389, ER-086526] and tritium-labeled eribulin (specific activity, 2.3×10^4 Ci/mol) were synthesized at Eisai Research Institute, Andover, MA (18).

Purification of Microtubule Protein and Tubulin

Bovine brain microtubule protein consisting of approximately 70% tubulin and 30% microtubule-associated proteins (MAPs) was purified without glycerol by three cycles of polymerization and depolymerization; tubulin was purified from the microtubule protein by phosphocellulose chromatography and stored at −70 °C as previously described (19). Immediately before each experiment, tubulin was thawed and cleared of aggregated protein by centrifugation at 66,000 × g for 30 min (4 °C). Protein concentration in all experiments was determined by Bradford assay with bovine serum albumin as the standard (20).

Eribulin Binding to Soluble Tubulin

Phosphocellulose-purified tubulin (1.8 μM) in PEM 50 buffer (50 mM PIPES, 1 mM EGTA, and 1 mM $MgSO_4$, pH 6.9) and 100 μM GTP was incubated with [^{3}H]eribulin (0.1 μM-70 μM) for 20 min at room temperature (22 °C), then 100 μL of each sample was added to a Zeba™ microspin desalting column (Thermo Fisher Scientific, Inc., Waltham, MA). Specific activity of each sample was measured immediately after eribulin addition. Columns were centrifuged for 2 min at 1500 × g following manufacturer's instructions. The protein content

and radioactivity in the tubulin flow-through were determined. Background radiolabel was assessed by centrifuging samples without protein at the concentrations of eribulin used. Background radioactivity levels correlated with eribulin concentration, with an average of 4.2% of the starting eribulin passing through the column with no protein present. This value was subtracted from all experimental radioactivity measurements.

Equilibrium binding data were quantified by measuring the fraction of tubulin bound with eribulin at various eribulin concentrations and a single fixed concentration of tubulin (2 μM). The following model for simple hyperbolic binding was fit to the data:

$$Y_D = Y_{max} D / (K_d + D)$$

In this model, D is the total concentration of eribulin, Y_D and Y_{max} are the ratios of bound eribulin to tubulin at subsaturating and infinite concentrations of D, respectively, and K_d is the equilibrium binding constant. The best-fit values for Y_{max} and K_d were determined by non-linear regression using KaleidaGraph® 3.5 (Synergy Software, Reading, PA). Y_{max} and K_d values and standard errors of eribulin binding to soluble tubulin were calculated using all data points as a single data set.

Microtubule Depolymerization

Microtubule depolymerization was measured by turbidity using a temperature-controlled Beckman Coulter (Fullerton, CA) spectrophotometer. Polymerization of MAP-rich tubulin (3 mg/ml) was initiated by incubation at 30°C for 30 min in PEM 100 buffer (100 mM PIPES, 1 mM EGTA, and 1 mM $MgSO_4$, pH 6.9) and 1 mM GTP. Microtubules were then sheared eight times through a 25 gauge needle and allowed to regain steady state for 15 min. Aliquots of microtubule suspension (100 μL) were added to cuvettes and placed in a warmed spectrophotometer at 30 °C. Eribulin (1 μM-20 μM) was added at time zero and absorbance readings were taken at a wavelength of 350 nm every minute for 30 min.

Dynamic Instability of Microtubule Minus Ends

The dynamic instability of microtubules in the presence of eribulin was measured as described previously (19,21,22). Briefly, microtubules (18 μM tubulin) were assembled from phosphocellulose-purified tubulin in PMEM buffer (86 mM PIPES, 26 mM MES, 1 mM EGTA, and 1.4 mM $MgSO_4$, pH 6.8) and 1 mM GTP in the presence or absence of eribulin. Microtubules were nucleated using sea urchin flagellar axonemal fragments and incubated at 35 °C for 30 min to achieve steady state. The behavior of individual microtubules was recorded by video-enhanced differential interference contrast microscopy with an IX71 Olympus (Melville, NY) inverted microscope and analyzed for growth and shortening events. Minus ends were distinguished from plus ends as described previously (23). Between 45 and 50 growth and shortening events were measured for each condition.

Eribulin Binding to Microtubules and Microtubule Length Determination

Microtubules were assembled from MAP-rich tubulin (3 mg/ml) and sheared to obtain a large number of short microtubules as described above, then incubated another 20 min to regain steady state. [^{3}H]Eribulin was added (0.1 μM-10 μM) to 375 μL of sheared microtubules and samples were immediately layered onto a microtubule stabilizing cushion (30% glycerol and 10% DMSO in PEM buffer) to minimize depolymerization at high eribulin concentrations (incubation time with drug was approximately 1-2 min). Microtubules were collected by centrifugation in an SW 50.1 swinging bucket rotor using a Beckman Coulter Optima ultracentrifuge (108,000 × g, 60 min, 30 °C). The soluble fraction was discarded, and microtubule pellets were carefully washed with PEM buffer and dissolved in 0.1 N NaOH at

4 °C overnight. Protein content and radioactivity of pellets were measured the following day. Background radiolabel was measured by performing parallel assays using 20 μM podophyllotoxin to inhibit microtubule polymerization (24). All results are reported with background subtracted.

Microtubule lengths were determined by electron microscopy (11) for use in determination of the stoichiometry of eribulin binding to microtubules. Lengths of a minimum of 300 microtubules were measured for each experiment. For controls, mean microtubule length ranged from 2.4 to 4.2 μm per experiment, with an overall mean of ~3 μm. Microtubules, either without eribulin addition for controls, or after eribulin incubation as described below, were fixed with 0.2% glutaraldehyde, placed on electron microscopy grids, stained with cytochrome *c* (1 mg/mL) and 1% uranyl acetate, and imaged using a JEOL 1230 transmission electron microscope (80 kV).

To account for eribulin-induced changes in microtubule length in stoichiometry determination, microtubules were incubated with the stated eribulin concentrations for 1-2 min and centrifuged through a DMSO/glycerol stabilizing cushion into a denser layer of 70% sucrose. Pelleted microtubules were fixed and stained as above and their lengths measured by electron microscopy. At concentrations of 5 and 10 μM, eribulin reduced the mean microtubule length by 17% and 29% respectively. These length changes were factored into the calculations of bound eribulin per microtubule for these two concentrations.

The number of eribulin molecules bound per microtubule was calculated using the mass and radioactivity of each pellet, the mean measured value for microtubule length, and the factor of 1,690 tubulin heterodimers per μm (25). Microtubules per liter was calculated for each sample using the microtubule pellet mass for that sample. Non-linear regression of binding data was computed using KaleidaGraph® 3.5 (Synergy Software) using the above equation. Y_{max} (ratio of bound eribulin molecules per microtubule) and K_d values for eribulin binding to microtubules were calculated for individual experiments, and the mean and standard error for all experiments was determined.

Effects of Vinblastine on Eribulin Binding to Microtubules

Unlabeled vinblastine (Sigma, St. Louis, MO) was added to sheared MAP-rich microtubules at a concentration of 2 μM or 4 μM for 15 min before [^{3}H]eribulin was added, then samples were treated as above. Electron microscopy samples for length measurements were taken after vinblastine incubation, but before eribulin addition. Consistent with previous findings that vinblastine stabilizes microtubule ends against shortening (11,19,26), in the presence of vinblastine (2 or 4 μM), eribulin induced no significant changes in microtubule length; therefore, the stoichiometry of eribulin bound per microtubule in the presence of vinblastine was calculated using the vinblastine-treated microtubule length measured in each experiment.

Morphology of Microtubule Ends

To determine drug effects on microtubule ends, unsheared microtubules were incubated with no drug, 50 μM eribulin or 50 μM vinblastine for 15 min, then 5 μL of sample was gently added to 15 μL glutaraldehyde (0.1% final concentration) on an electron microscope grid and stained as above. Both ends of 50 microtubules each for control and eribulin-treated microtubules and 30 microtubules for vinblastine-treated microtubules were examined and categorized as blunt, slightly splayed, or extensively splayed/spiraled.

RESULTS

Eribulin Binds a Single Site on α/β-Tubulin Heterodimers

We measured the binding stoichiometry of [^{3}H]eribulin to soluble bovine brain tubulin using centrifugal gel filtration. [^{3}H]eribulin was incubated with tubulin (2 μM, 20 min, 30 °C), then bound and free drug were separated by centrifugation using a microspin gel column (Materials and Methods) and the stoichiometry of eribulin bound to tubulin was determined. The binding curve is complex (shown on a logarithmic scale in Fig. 1B). To simplify the interpretation, we analyzed eribulin binding for concentrations ≤ 10 μM and ≥ 10 μM as two separate data sets. At low concentrations (0.1-10 μM), binding reached a plateau when approximately 25% of the tubulin was bound, with a Y_{max} of 0.26 ± 0.02 and a K_d of 0.4 ± 0.2 μM (determined by fitting the points ≤ 10 μM eribulin to the hyperbolic binding equation presented in Materials and Methods). Between 10 and 30 μM eribulin, binding increased sharply and approached saturation, as indicated by the change in slope of the curve. At 70 μM, the stoichiometry was 0.8 eribulin molecules per tubulin dimer. At concentrations > 70 μM, data were highly scattered (not shown), likely due to high background. Overall, eribulin bound soluble tubulin with a Y_{max} of 1.3 ± 0.4 eribulin molecules per heterodimer and a K_d of 46 ± 28 μM eribulin (determined by fitting the points ≥ 10 μM eribulin to the equation in Materials and Methods) (Fig. 1C).

Eribulin-Induced Depolymerization of Microtubules

Eribulin (1-20 μM) was added to steady-state MAP-rich microtubules and changes in microtubule polymer mass were examined by turbidity for 30 min (Fig. 2A). Microtubules underwent an immediate, but partial, depolymerization in the first minute. By 30 min, microtubule polymer mass had relaxed to a new steady state. The final extent of depolymerization increased in a linear, concentration dependent manner (Fig. 2B) ($R^2 = 0.96$). At 30 min, there was a 4.5% decrease in polymer mass at 1 μM eribulin and an 80% decrease at 20 μM eribulin. Fifty percent reduction in polymer mass occurred at 11 μM eribulin.

Eribulin Does Not Affect Dynamic Instability at Microtubule Minus Ends

Previous results indicated that eribulin inhibits dynamic instability at microtubule plus ends (11) but the effects on minus ends had not been determined. Microtubules were assembled at 35 °C using sea urchin axoneme nucleating seeds, recorded for 10 min by video enhanced differential interference contrast microscopy, and the dynamic instability at microtubule minus ends was analyzed (Materials and Methods). As shown in Table 1, in the absence of eribulin, minus ends of microtubules were less dynamic than plus ends. In contrast to the eribulin-induced suppression of growth rates and lengths at plus ends (46% and 50%, respectively), 100 nM eribulin had no significant effect on any parameters of dynamic instability at minus ends.

Eribulin Binds to Microtubule Ends at a Maximum Stoichiometry of ~15 Eribulin Molecules per Microtubule

To examine the binding of eribulin to microtubules, MAP-rich microtubules were polymerized to steady state, sheared to increase the number of microtubule ends, incubated with [^{3}H]eribulin (0.1 μM-10 μM) for 1-2 min, and collected by centrifugation through a glycerol/DMSO stabilizing cushion.

By calculating the eribulin bound per microtubule using the eribulin and tubulin content of each pellet and the mean microtubule length (Materials and Methods), we found that eribulin bound to microtubules in a concentration-dependent manner, as shown in Fig. 3A and as a double reciprocal plot in Fig. 3B. At the lowest eribulin concentration (0.1 μM), an average of

0.48 eribulin molecules bound per microtubule. The stoichiometry increased to a value of 6.1 eribulin per microtubule at 2 μM, above which binding approached saturation, as indicated by a change in the slope of the curve. At 10 μM, binding was 11 eribulin per microtubule. Non-linear regression analysis (Materials and Methods) indicated that eribulin binds to microtubules with a Y_{max} of 14.7 ± 1.3 eribulin per microtubule and a K_d of 3.5 ± 0.6 μM eribulin. The low binding maximum is indicative of binding to microtubule ends, where there is an average of 13 tubulin dimers exposed at each end (25).

Vinblastine Inhibits the Binding of < 5 μM Eribulin and Enhances the Binding of > 5 μM Eribulin to Microtubule Ends In Vitro

To study the eribulin binding site and its location relative to the vinca domain, we examined the influence of vinblastine on eribulin binding to microtubules. Vinblastine (2 or 4 μM) was added to sheared, steady-state, MAP-rich microtubules for 15 min before adding [^{3}H]eribulin (0.1 μM-10 μM). Microtubule lengths were determined, and after centrifugation through a glycerol/DMSO cushion and determination of tubulin mass and bound eribulin in the pellets, the number of eribulin molecules bound per microtubule was calculated (Fig. 4A).

The results for the low eribulin concentration range (0.1-2 μM) are shown enlarged in Fig. 4B. Vinblastine inhibited eribulin binding at low eribulin concentrations, consistent with previous findings with soluble tubulin (2,10). At the lowest eribulin concentration, vinblastine (2 μM) inhibited binding of eribulin (0.1 μM) to microtubules by 44% (from 0.48 ± 0.06 to 0.27 ± 0.05 eribulin molecules per microtubule ± SEM). Surprisingly, the extent of inhibition decreased as the eribulin concentration was increased; 2 μM vinblastine inhibited 5 μM eribulin slightly but the change in eribulin per microtubule was not significant (from 8.7 ± 1.1 to 8.1 ± 0.72). At 10 μM eribulin, 2 μM vinblastine increased eribulin binding by 36% (from 11 ± 1.2 to 15 ± 1.1). These unique effects were further enhanced at 4 μM vinblastine: the binding of 0.1 μM eribulin was reduced by 63% (from 0.48 ± 0.06 to 0.18 ± 0.004), the binding of 5 μM eribulin was reduced only slightly and not significantly (from 8.7 ± 1.1 to 7.8 ± 0.33), and the binding of 10 μM eribulin was increased by 55% (from 11 ± 1.2 to 17 ± 1.7).

Effects of Eribulin on Microtubule Structure Differ from those of Vinblastine

Microtubule ends after incubation of MAP-rich microtubules with 50 μM eribulin or 50 μM vinblastine are shown in Fig. 5. The ends of the control and eribulin-treated microtubules were blunt or slightly splayed; however, no extensively splayed or spiraled protofilaments occurred (Fig. 5A, B). In contrast, all of the vinblastine-treated microtubules had extremely splayed ends, many with long, spiraled protofilaments emanating from one or both ends (Fig. 5C). The structures of the microtubule ends were examined for control, eribulin-treated, and vinblastine-treated microtubules (Table 2). 50 microtubules were counted for control and eribulin-treated microtubules, and 30 microtubules were counted for vinblastine-treated microtubules. The majority (72%) of control microtubules showed no splaying at either end, compared with 34% of eribulin-treated microtubules. A single end was slightly splayed in 44% of eribulin-treated microtubules, and 22% had both ends slightly splayed, compared with 24% and 4% of control microtubules, respectively. In contrast, all of the vinblastine-treated microtubules were splayed or spiraled at both ends, and most of them (80%) were extensively splayed or spiraled at both ends, whereas none of the eribulin-treated microtubules showed this morphology at either end.

DISCUSSION

We found that eribulin binds to a single site on soluble tubulin with low affinity and to a very small number of sites at microtubule ends with high affinity. The binding to soluble tubulin is complex with an intermediate plateau occurring at ≤ 10 μM eribulin with a stoichiometry of 0.26 ± 0.02 eribulin/tubulin dimer with an apparent very high affinity (K_d, 0.4 ± 0.2 μM)

(discussed further below). At higher eribulin concentrations the drug bound 1.3 ± 0.4 saturable low affinity sites per tubulin dimer (K_d, 46 ± 28 μM). Eribulin bound with high affinity (K_d, 3.5 ± 0.6 μM) to 14.7 ± 1.3 saturable sites per microtubule, indicating high affinity binding to microtubule ends. Eribulin had no significant effect on dynamic instability at microtubule minus ends in contrast to its potent suppression of growth rates and lengths at plus ends. When added to steady-state MAP-rich microtubules, eribulin induced an immediate transient depolymerization proportional to the eribulin concentration, before attaining a new steady state polymer mass. In the presence of vinblastine, eribulin binding to microtubules was inhibited at ≤ 5 μM eribulin, but above 5 μM, eribulin binding was increased.

The reason for the complex nature of the binding to soluble tubulin (Fig. 1B) is not clear. We found that a plateau in the binding occurred between 1 and 10 μM eribulin with only ~25% of the tubulin bound. At concentrations above 10 μM, eribulin bound the remainder of the tubulin, with complete saturation at slightly higher than a 1:1 ratio of eribulin to tubulin. There are at least three conceivable explanations for the intermediate plateau in the binding isotherm. One explanation might be differing affinities of eribulin for binding to different tubulin isotypes. Bovine brain tubulin contains a mixture of several tubulin isotypes of which $\alpha\beta_{III}$ tubulin is approximately 25% of the total (27) and is therefore a candidate for such putative high affinity eribulin binding. It is also formally conceivable that there are two eribulin binding sites on the β_{III} tubulin molecule, one of high affinity and the second of lower affinity thus yielding a maximal overall stoichiometry of 1.3 eribulin molecules/tubulin, although we consider this unlikely. The third possibility is that the plateau in the binding isotherm is artifactual. Tubulin tends to self associate and form oligomers, and this is largely inhibited by eribulin (28). Since eribulin does not appear to bind with significant affinity to the sides of microtubules, it is conceivable that at lower eribulin concentrations (≤ 10 μM), tubulin oligomerization competes for the eribulin binding site causing an artifactual plateau in the isotherm, a phenomenon that would be negated at higher eribulin concentrations. To discern among the potential causes will require further experimentation.

The addition of eribulin to MAP-rich microtubules induced a rapid transient depolymerization before a new reduced steady-state polymer mass was attained (Fig. 2A). Half-maximal depolymerization of microtubules occurred at 11 μM eribulin; at this concentration 11 eribulin molecules were bound per microtubule. The extent of depolymerization after 30 min (Fig. 2B) was directly proportional to the eribulin concentration, suggesting that a depletion of the soluble tubulin pool by binding to eribulin is directly responsible for the decrease in polymer mass. The number of microtubule ends was approximately 5 nM, while the soluble tubulin concentration was much higher, equaling approximately 40% of the total tubulin concentration in the control, or ~8 μM. Therefore, although the K_d for eribulin binding to soluble tubulin is more than 10 × higher than for tubulin in microtubules, the concentration of soluble tubulin is over 1,000 times higher than the concentration of microtubules ends, resulting in a significant portion of eribulin binding to soluble tubulin as well as to microtubule ends.

The depolymerization may at first appear contradictory to our previous finding that, at steady state, low concentrations of eribulin (100 nM) suppressed the growth rate of microtubule dynamic instability but had no significant effect on the shortening rate (11). However, in explanation, when eribulin is added to microtubules, it binds to tubulin in the soluble pool, reducing the amount of free soluble tubulin available to add to the microtubule ends and thus upsetting the steady-state equilibrium between dynamic microtubules and soluble tubulin. Sufficient tubulin must then be lost from the microtubules by depolymerization to re-establish a new steady state.

Eribulin bound a maximum of 15 sites per microtubule (Fig. 3). Saturation at such a low number of drug molecules per microtubule strongly indicates binding at microtubule ends.

Microtubules contain a small number of exposed tubulin dimers at each end, between 12-14 per end, versus nearly 2000 potential binding sites per micrometer of length along the microtubule lattice (25). These data suggest that eribulin binds to only one end of a microtubule, since binding to both ends would likely result in a higher binding maximum. These binding sites in microtubules had high affinity for eribulin, more than 10 × higher than the affinity of eribulin for binding to soluble tubulin suggesting that the primary mechanism of eribulin is to bind to microtubule ends to exert its effect.

Eribulin potently inhibited microtubule plus end growth by 46-50% (Table 1 and (11)) when only 0.5 eribulin molecules were bound per microtubule (at 100 nM eribulin, Fig. 3). Thus, the binding of a single eribulin molecule at the end of a microtubule can strongly inhibit microtubule growth. It is likely that the binding of eribulin or an eribulin-tubulin complex to a microtubule end may sterically hinder the addition of new tubulin dimers to growing protofilaments.

At 100 nM eribulin there was no significant change in microtubule dynamic instability at minus ends (Table 1). The evidence indicating that eribulin preferentially suppresses plus end dynamic instability, and that eribulin binds to a maximum of 15 sites per microtubule, strongly suggests that eribulin binds primarily at the plus ends of microtubules. These data, together with the result that eribulin binds α/β tubulin heterodimers at a single site (Fig. 1C), suggest that the β-tubulin subunit contains the major portion of the eribulin binding site. These data are in agreement with recent results from Alday and Correia (2009) (28) suggesting that eribulin does not bind to both α- and β-tubulin, but binds to either the interdimer interface or to the β-tubulin subunit alone.

By electron microscopy, we showed that eribulin at high concentration (50 μM) did not induce extensive protofilament spiraling at microtubule ends as occurs with vinblastine (Fig. 5). The ends of the microtubules were blunt or slightly splayed (Table 2). This finding supports the model that eribulin binds β-tubulin with high affinity and α-tubulin with low or no affinity, and thus eribulin does not “link” tubulin heterodimers together in the manner of vinblastine, which binds both subunits nearly equally (17). However, the presence of the slightly splayed microtubule ends suggests a possible low affinity binding to α-tubulin. Since 22% of eribulin-treated microtubules showed slight splaying at both ends, therefore it appears that at sufficiently high concentrations, eribulin may bind minus ends.

Vinblastine inhibited eribulin binding to microtubules at low eribulin concentrations (≤ 5 μM), (Fig. 4A and B). Unexpectedly, vinblastine induced an increase in the number of eribulin binding sites per microtubule at higher eribulin concentrations, increasing from 11 to 14 and to 17 eribulin molecules per microtubule in the presence of 2 μM and 4 μM vinblastine, respectively (Fig. 4A). This slight increase in binding suggests that the vinblastine-induced splaying of protofilaments allows increased access of eribulin to additional sites at the microtubule end (29).

Acknowledgments

We thank Mr. Herb Miller for expert purification of bovine brain tubulin and Dr. John Lew and Dr. John Correia for valuable discussions of the binding analysis.

Abbreviations

DMSO	dimethyl sulfoxide
EGTA	ethylene glycol tetraacetic acid
GTP	guanosine-5′-triphosphate

MAP	microtubule-associated protein
MES	2-(N-morpholino)ethanesulfonic acid
PIPES	1,4 piperazine bis (2-ethanosulfonic acid)
SEM	standard error of the mean

REFERENCES

1. Towle MJ, Salvato KA, Budrow J, Wels BF, Kuznetsov G, Aalfs KK, Welsh S, Zheng W, Seletsk BM, Palme MH, Habgood GJ, Singer LA, Dipietro LV, Wang Y, Chen JJ, Quincy DA, Davis A, Yoshimatsu K, Kishi Y, Yu MJ, Littlefield BA. In vitro and in vivo anticancer activities of synthetic macrocyclic ketone analogues of halichondrin B. Cancer Res 2001;61:1013–1021. [PubMed: 11221827]
2. Dabydeen DA, Burnett JC, Bai RL, Verdier-Pinard P, Hickford SJH, Pettit GR, Blunt JW, Munro MHG, Gussio R, Hamel E. Comparison of the activities of the truncated halichondrin B analog NSC 707389 (E7389) with those of the parent compound and a proposed binding site on tubulin. Molecular Pharmacology 2006;70:1866–1875. [PubMed: 16940412]
3. Hirata Y, Uemura D. Halichondrins - Antitumor Polyether Macrolides from a Marine Sponge. Pure and Applied Chemistry 1986;58:701–710.
4. Goel S, Mita AC, Mita M, Rowinsky EK, Chu QS, Wong N, Desjardins C, Fang F, Jansen M, Shuster DE, Mani S, Takimoto CH. A Phase I Study of Eribulin Mesylate (E7389), a Mechanistically Novel Inhibitor of Microtubule Dynamics, in Patients with Advanced Solid Malignancies. Clinical Cancer Research 2009;15:4207–4212. [PubMed: 19509177]
5. Tan AR, Rubin EH, Walton DC, Shuster DE, Wong YN, Fang F, Ashworth S, Rosen LS. Phase I study of eribulin mesylate administered once every 21 days in patients with advanced solid tumors. Clin Cancer Res 2009;15:4213–4219. [PubMed: 19509146]
6. Vahdat LT, Pruitt B, Fabian CJ, Rivera RR, Smith DA, Tan-Chiu E, Wright J, Tan AR, DaCosta NA, Chuang E, Smith J, O'Shaughnessy J, Shuster DE, Meneses NL, Chandrawansa K, Fang F, Cole PE, Ashworth S, Blum JL. Phase II Study of Eribulin Mesylate, a Halichondrin B Analog, in Patients With Metastatic Breast Cancer Previously Treated With an Anthracycline and a Taxane. Journal of Clinical Oncology 2009;27:2954–2961. [PubMed: 19349550]
7. Postma TJ, Vermorken JB, Liefting AJ, Pinedo HM, Heimans JJ. Paclitaxel-induced neuropathy. Ann Oncol 1995;6:489–494. [PubMed: 7669713]
8. Pace A, Bove L, Nistico C, Ranuzzi M, Innocenti P, Pietrangeli A, Terzoli E, Jandolo B. Vinorelbine neurotoxicity: clinical and neurophysiological findings in 23 patients. J Neurol Neurosurg Psychiatry 1996;61:409–411. [PubMed: 8890782]
9. Quasthoff S, Hartung HP. Chemotherapy-induced peripheral neuropathy. J Neurol 2002;249:9–17. [PubMed: 11954874]
10. Bai R, Paull KD, Herald CL, Malspeis L, Pettit GR, Hamel E. Halichondrin-B and Homohalichondrin-B, Marine Natural-Products Binding in the Vinca Domain of Tubulin - Discovery of Tubulin-Based Mechanism of Action by Analysis of Differential Cytotoxicity Data. Journal of Biological Chemistry 1991;266:15882–15889. [PubMed: 1874739]
11. Jordan MA, Kamath K, Manna T, Okouneva T, Miller HP, Davis C, Littlefield BA, Wilson L. The primary antimitotic mechanism of action of the synthetic halichondrin E7389 is suppression of microtubule growth. Molecular Cancer Therapeutics 2005;4:1086–1095. [PubMed: 16020666]
12. Okouneva T, Azarenko O, Wilson L, Littlefield BA, Jordan MA. Inhibition of centromere dynamics by eribulin (E7389) during mitotic metaphase. Molecular Cancer Therapeutics 2008;7:2003–2011. [PubMed: 18645010]
13. Jordan MA, Kamath K. How do microtubule-targeted drugs work? An overview. Curr Cancer Drug Tar 2007;7:730–742.
14. Jordan MA, Wilson L. Microtubules as a target for anticancer drugs. Nature Reviews Cancer 2004;4:253–265.

15. Cormier A, Marchand M, Ravelli RBG, Knossow M, Gigant B. Structural insight into the inhibition of tubulin by vinca domain peptide ligands. Embo Reports 2008;9:1101–1106. [PubMed: 18787557]
16. Hamel E. Natural-Products Which Interact with Tubulin in the Vinca Domain - Maytansine, Rhizoxin, Phomopsin-a, Dolastatin-10 and Dolastatin-15 and Halichondrin-B. Pharmacology & Therapeutics 1992;55:31–51. [PubMed: 1287674]
17. Gigant B, Wang C, Ravelli RB, Roussi F, Steinmetz MO, Curmi PA, Sobel A, Knossow M. Structural basis for the regulation of tubulin by vinblastine. Nature 2005;435:519–522. [PubMed: 15917812]
18. Littlefield, BA.; Palme, M.; Seletsky, BM.; Towle, MJ.; Melvin, YJ.; Zheng, W. Macrocyclic analogs and methods of their use and preparation. Eisai Co. Ltd.; 2001.
19. Toso RJ, Jordan MA, Farrell KW, Matsumoto B, Wilson L. Kinetic stabilization of microtubule dynamic instability in vitro by vinblastine. Biochemistry 1993;32:1285–1293. [PubMed: 8448138]
20. Bradford MM. A rapid and sensitive method for the quantitation of microgram quantities of protein utilizing the principle of protein-dye binding. Anal Biochem 1976;72:248–254. [PubMed: 942051]
21. Panda D, Goode BL, Feinstein SC, Wilson L. Kinetic stabilization of microtubule dynamics at steady state by tau and microtubule-binding domains of tau. Biochemistry 1995;34:11117–11127. [PubMed: 7669769]
22. Walker RA, O'Brien ET, Pryer NK, Soboeiro MF, Voter WA, Erickson HP, Salmon ED. Dynamic instability of individual microtubules analyzed by video light microscopy: rate constants and transition frequencies. J Cell Biol 1988;107:1437–1448. [PubMed: 3170635]
23. Derry WB, Wilson L, Jordan MA. Low potency of taxol at microtubule minus ends: implications for its antimitotic and therapeutic mechanism. Cancer Res 1998;58:1177–1184. [PubMed: 9515803]
24. Loike JD, Brewer CF, Sternlicht H, Gensler WJ, Horwitz SB. Structure-activity study of the inhibition of microtubule assembly in vitro by podophyllotoxin and its congeners. Cancer Res 1978;38:2688–2693. [PubMed: 679171]
25. Amos L, Klug A. Arrangement of subunits in flagellar microtubules. J Cell Sci 1974;14:523–549. [PubMed: 4830832]
26. Jordan MA, Wilson L. Kinetic analysis of tubulin exchange at microtubule ends at low vinblastine concentrations. Biochemistry 1990;29:2730–2739. [PubMed: 2346745]
27. Banerjee A, Roach MC, Wall KA, Lopata MA, Cleveland DW, Luduena RF. A monoclonal antibody against the type II isotype of beta-tubulin. Preparation of isotypically altered tubulin. J Biol Chem 1988;263:3029–3034. [PubMed: 3277964]
28. Alday PH, Correia JJ. Macromolecular Interaction of Halichondrin B Analogues Eribulin (E7389) and ER-076349 with Tubulin by Analytical Ultracentrifugation. Biochemistry. 2009
29. Wilson L, Jordan MA, Morse A, Margolis RL. Interaction of vinblastine with steady-state microtubules in vitro. J Mol Biol 1982;159:125–149. [PubMed: 7131559]
30. Wilson, L.; Jordan, MA. Pharmacological Probes of Microtubule Function. John Wiley and Sons; New York: 1994.
31. Wilson L, Creswell KM, Chin D. The mechanism of action of vinblastine. Binding of [acetyl-3H] vinblastine to embryonic chick brain tubulin and tubulin from sea urchin sperm tail outer doublet microtubules. Biochemistry 1975;14:5586–5592. [PubMed: 1203244]

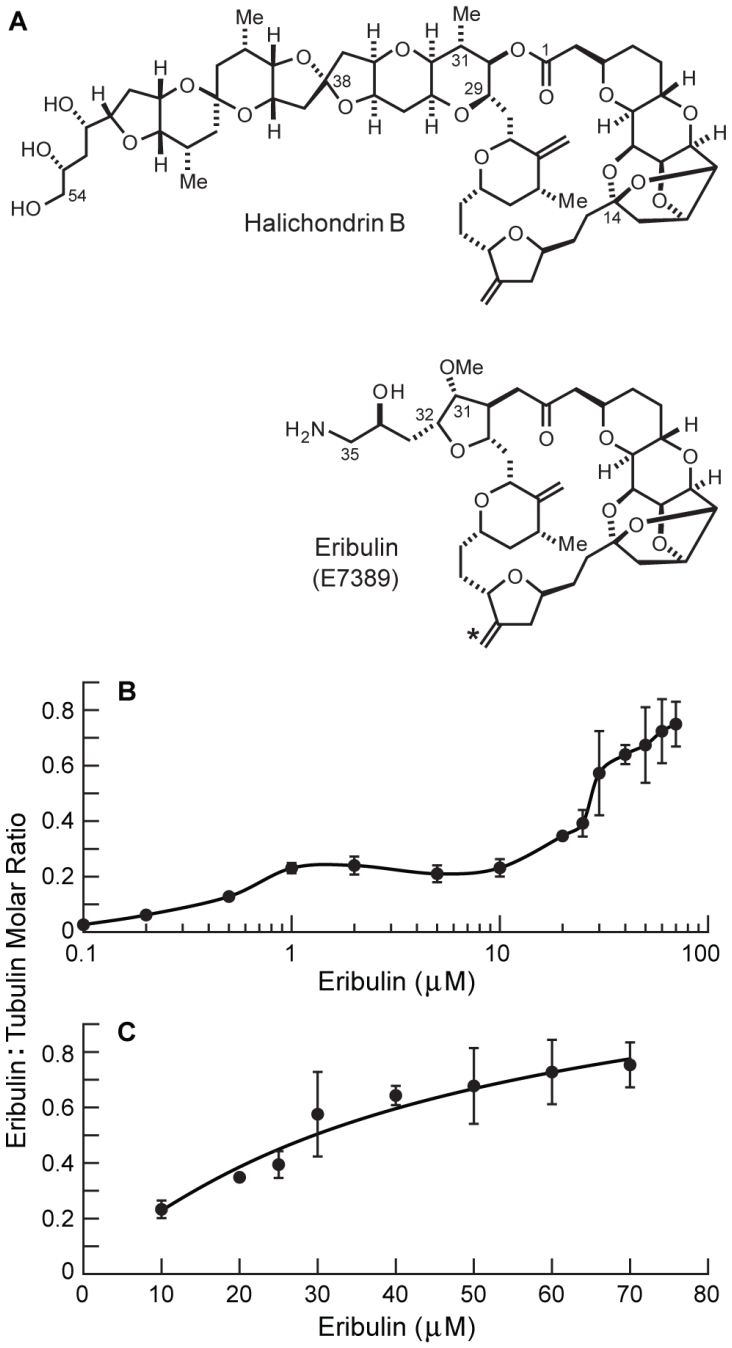

Figure 1.

(A) Eribulin (E7389) and its parent compound halichondrin B. The location of tritiation in [^{3}H]eribulin is indicated by an asterisk (*). (B) Binding of eribulin to soluble tubulin. (C) Enlargement of (B) showing the binding of eribulin to soluble tubulin with the curve determined by non-linear regression. [^{3}H]Eribulin was incubated with soluble MAP-depleted bovine brain tubulin (2 μM) for 20 min at 30 °C, followed by centrifugation through a microspin gel filtration column. Data are means ± SEM of three to six experiments.

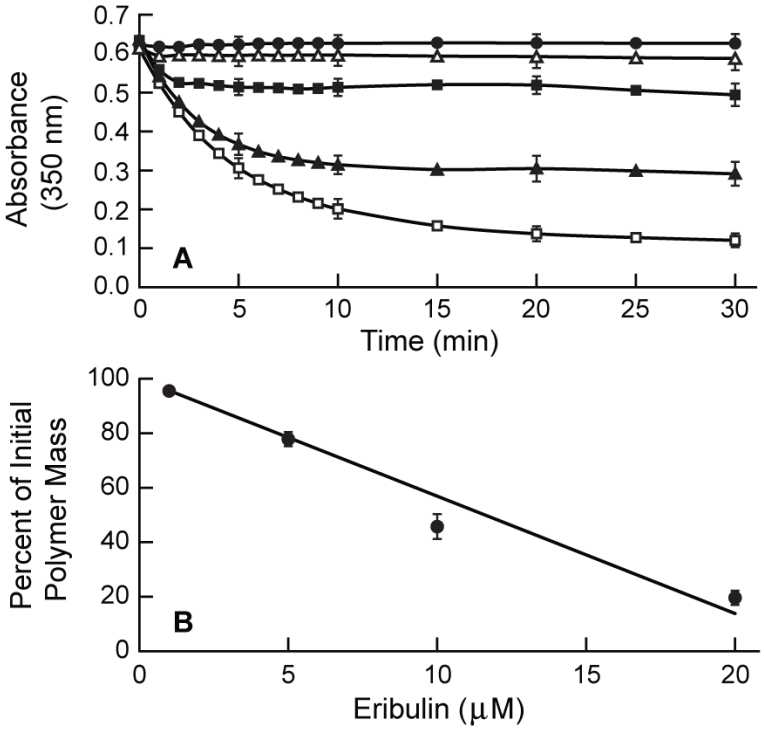

Figure 2.

Eribulin-induced depolymerization of MAP-rich microtubules. (A) Control (solid circle), 1 μM (open triangle), 5 μM (solid square), 10 μM (solid triangle), and 20 μM eribulin (open square). (B) Extent of final depolymerization at 30 min after eribulin addition. MAP-rich tubulin (3 mg/ml) was assembled to steady state, eribulin was added at time zero and depolymerization was followed by turbidity (A350 nm). Data are means ± SEM of four to five experiments.

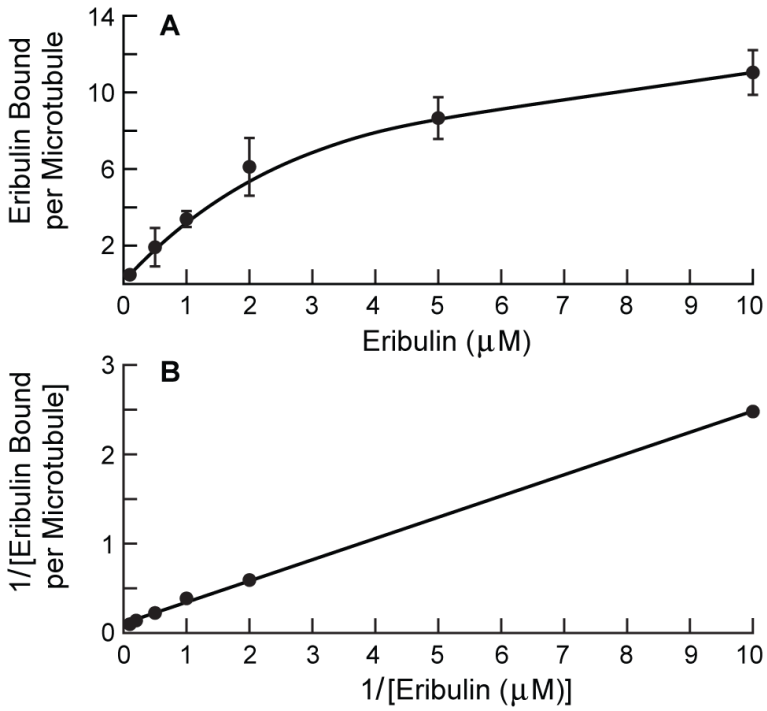

Figure 3.

Binding of eribulin to microtubules. (A) Eribulin binds microtubules at a maximum of ~15 molecules/microtubule. (B) Double-reciprocal plot of eribulin binding to microtubules of a representative experiment ($R^2 = 0.99$). MAP-rich tubulin (3 mg/ml) was assembled to steady state, then incubated with [^{3}H]eribulin for 1-2 min, followed by centrifugation through a stabilizing cushion. Data are means ± SEM of four experiments.

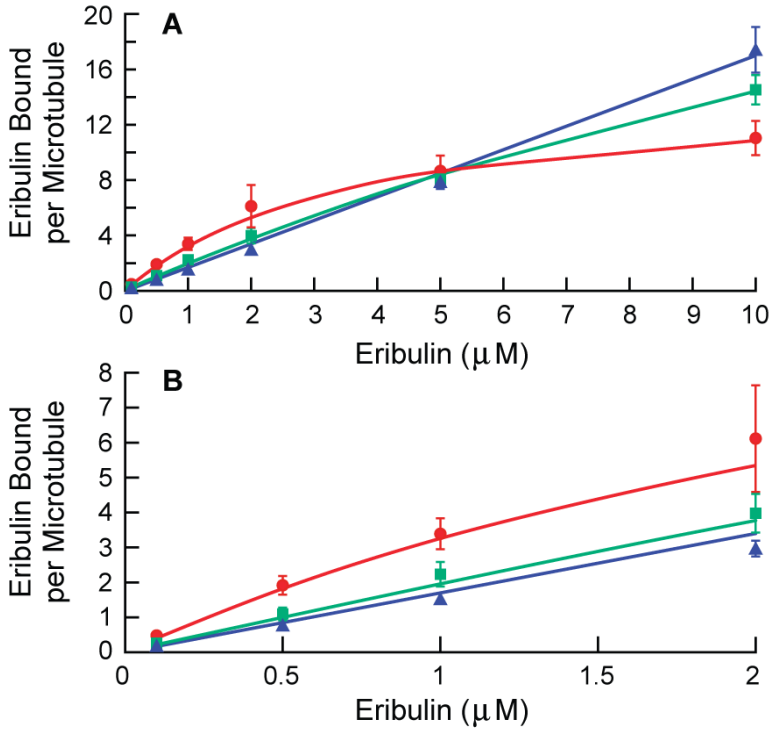

Figure 4.

Effects of vinblastine on eribulin binding to microtubules. (A) Vinblastine inhibited eribulin binding at low eribulin concentrations, but increased binding at high eribulin concentrations. (B) Enlargement of (A) showing effects of vinblastine at low eribulin concentrations. Vinblastine was added to microtubules and incubated for 15 min before [^{3}H]eribulin was added. Eribulin binding in the absence of vinblastine (red circles), and in the presence of 2 μM vinblastine (green squares) and 4 μM vinblastine (blue triangles). Non-linear regression (Materials and Methods) was used to generate the curves for control and 2 μM vinblastine; a simple linear equation was used for 4 μM vinblastine.

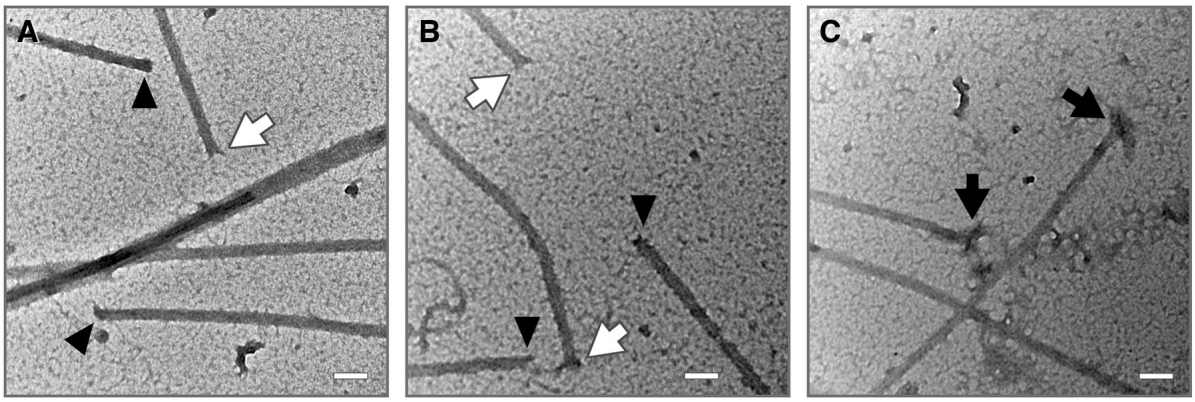

Figure 5.

Electron micrographs of microtubules after incubation with (A) no drug, (B) 50 μM eribulin or (C) 50 μM vinblastine. Ends in controls or eribulin-treated microtubules were either blunt (*black triangles*) or splayed (*white arrows*). After incubation with vinblastine, all ends were extensively splayed and many had protruding spiraled protofilaments (*black arrows*). Magnification 100,000 ×, scale bar 100 nm.

Table 1

Plus and minus end microtubule dynamic instability in the presence of 100 nM eribulin

		Plus End[a]			Minus End	
	Control	**Eribulin, 100 nM**	**Percent Change**	**Control**	**Eribulin, 100 nM**	**Percent Change**
Growth rate (μm/min)	0.9 ± 0.1[b]	0.5 ± 0.04	−46[c]	0.6 ± 0.1	0.6 ± 0.02	ns
Growing length (μm)	2.4 ± 0.3	1.2 ± 0.2	−50	0.9 ± 0.1	0.8 ± 0.1	ns
Shortening rate (μm/min)	33 ± 1.9	24 ± 1.9	*d*	14 ± 1.7	18 ± 3.7	ns
Shortening length (μm)	5.9 ± 0.5	3.7 ± 0.4	*d*	2.7 ± 0.4	3.5 ± 0.2	ns
Time growing (%)	85	74		28	25	
Time shortening (%)	5	5		9	11	
Time attenuated (%)	10	21		63	64	
Catastrophe frequency per min	0.3	0.3	ns[e]	0.2	0.4	ns
Rescue frequency per min	2.4	2.2	ns	2.3	1.9	ns
Dynamicity	2.4	1.4	−40	0.4	0.5	

[a] Plus end data were previously reported in Jordan et al. (11).

[b] ± SEM.

[c] Values were considered significant from controls at the 99% confidence levels by Student's t test.

[d] Shortening rates in the presence of drug were not considered reliable because of the artificially reduced shortening lengths due to the shorter overall lengths of the microtubules.

[e] ns, not significant.

Table 2

Structure of microtubule ends in the absence of drug or in the presence 50 μM eribulin or 50 μM vinblastine

	Control[a]	Eribulin, 50 μM	Vinblastine, 50 μM
Both ends blunted	72%	34%	
One end slightly splayed, one end blunted	24%	44%	
Both ends slightly splayed	4%	22%	
One end slightly splayed, one end extensively splayed or spiraled			20%
Both ends extensively splayed or spiraled			80%

[a] 50 microtubules were examined for control and eribulin-treated microtubules, 30 microtubules were examined for vinblastine-treated microtubules.